Research Article

Antonio Gagliano, Francesco Nocera, Andrea Cicero, Luigi Marletta, and Gianpiero Evola*

Mitigation of environmental noise in urban streets through lightweight transparent screens

https://doi.org/10.1515/noise-2020-0005
Received Sep 16, 2019; accepted Mar 20, 2020

Abstract: Noise pollution is one of the main environmental stressors in urban areas. In particular, strong noise pollution can be experienced at nighttime in downtown areas with intense anthropic activities: here, dwellers may suffer from disturbance to their rest, which induces stress and – in turn – adverse effects on health.
Usually, local authorities implement actions to tackle noise pollution, *e.g.* limiting the time allowed for outdoor events. However, these measures are often inadequate because the noise annoyance comes directly by the shouting of people spending time outdoors till late night.
In this framework, this study proposes a procedure to optimize the shape of customized lightweight transparent noise screens that can be applied to façades in order to reduce noise disturbance in urban canyons. The case study of the "movida" area in the downtown of Marina di Ragusa (Southern Italy) is discussed to test the applicability of the proposed procedure.
The results of this analysis allow defining the shape and the size of the noise screens that minimize the noise annoyance perceived by residents. The proposed mitigation approach can be applied in cities affected by significant noise pollution.

Keywords: noise pollution, noise screens, urban canyons, genetic algorithms, parametric design

***Corresponding Author: Gianpiero Evola:** DIEEI, University of Catania, Viale A. Doria 6, 95125 Catania, Italy; Email: gevola@unict.it
Antonio Gagliano, Luigi Marletta: DIEEI, University of Catania, Viale A. Doria 6, 95125 Catania, Italy
Francesco Nocera: DICAr, University of Catania, Via Santa Sofia 64, 95123 Catania, Italy
Andrea Cicero: Gillieron Scott Acoustic Design, 130 Brixton Hill, SW2 1RS London, United Kingdom of Great Britain and Northern Ireland

1 Introduction

Environmental noise, generated by human activities, is a relevant environmental issue in densely populated areas [1]. Indeed, European Union estimates that around 20% of European population suffer from noise exposure. Moreover, according to a study conducted by the World Health Organization, environmental noise has been ranked in six European cities as the second main environmental stressor that affects public health, and the expected trend is that noise exposure is going to increase in Europe compared to other stressors [2].

The composition of urban noise is complex, due to a wide range of sounds originated by different sources, such as transport (road traffic, aircraft and railway noise), commercial and entertainment activities [3]. It is commonly known that road traffic noise in urban areas severely affects people's health and lives [4], since it often exceeds tolerance levels. However, in city centres and in crowded touristic areas, where the concentration of anthropic activities is rather high, very high noise levels may also be experienced because of recreational activities (the so-called *movida*), especially during nighttime. This causes sleep disturbance for residents, which in turn may even induce serious consequences on wellness [5].

Some studies in the literature have already tackled the issue of recreational noise in urban areas. As an example, Ottoz *et al.* [6] examined the case of some "movida" districts in Milan and Turin. By means of online questionnaires, residents reported that the high noise levels, coming from shouts and music due to outdoor events or to public places, affect their sleep, everyday life and health; they were also concerned about estate depreciation and expenses to mitigate the problem. The sound level measurements in some samples confirmed what the residents declared, showing very high sound pressure levels in the residents' homes between 11 p.m. and 02 a.m., both with open and closed windows.

On the other hand, Ballesteros *et al.* developed a procedure for the noise characterization of leisure areas, and investigated three leisure areas of a big-sized city (Madrid) and one of a medium-sized city (Cuenca) in Spain [7]. The

results allowed to determine typical spatiotemporal patterns of the sound pressure levels in leisure areas, and confirmed that the main source of noise is people shouting in the streets.

Now, there are basically three types of mitigation actions for noise pollution in densely built areas:

- action on the disturbing source, by reducing its emission levels;
- action on the receivers, by relocating residential buildings far from noisy areas;
- use of anti-noise devices.

However, when dealing with noise coming from recreational activities in city centres, the installation of anti-noise devices is by far the most feasible solution. One could also think to forbid or put strict limitations to these activities, which however offer important opportunities for employment and income.

Amongst anti-noise devices in urban areas, noise barriers are probably the most common solutions and constantly receive significant attention, as reported in [8, 9]. The effectiveness of a noise barrier to attenuate environmental noise depends on its geometry and its position relative to the source and the receiver; therefore, experimental studies are often focused on optimizing barrier shape to get high performance [10].

Noise barriers are frequently used to deal with traffic noise; on the contrary, their use to deal with noise coming from leisure activities and people shouting in the streets, in a dense urban environment, is much less common. In fact, they are less effective in urban canyons, where they cannot effectively intercept the sound waves reaching the receivers by reflection on the façades. Moreover, they are liable to alter the visual context, especially for local residents.

With reference to this issue, one interesting solution can be the adoption of transparent lightweight screens. On the market there are already several products that could be used to this purpose: all of them consist in polycarbonate sheets with certified resistance to wind load and impact load, UV protection to avoid weathering, chemical and abrasion resistance, low weight (around 12 kg/m^2), high transparency to light (around 88%) and flame retardant properties (*i.e.* self-estinguishing). These panels are commonly used as vertical noise screens: their thickness is between 8 and 12 mm, and they are produced in many different shapes (even curved ones). With few modifications, they could be easily adapted to the purposes of this study.

Some researchers also investigated the effectiveness of eaves and louvers [13], and concluded that eaves placed above the position of a potential receiver should be inclined in order to avoid sound reflection towards the building façade [14]. Vertical greenery systems applied to building façades can also be useful to counteract reverberation within urban canyons [15].

An innovative approach to the design of lightweight noise screens in urban areas consists in the use of Genetic Algorithms (GA) [16]. Nowadays, GAs are widely used in the architectural and construction industry in order to identify the best geometry and shape of an object to fulfil a specific function, such as structural resistance, energy savings and acoustic performance [17, 18]. Some remarkable works using GAs in shape optimization for noise barriers can be found in the literature [19–25]. However, no study investigated this issue in the "movida" areas.

In this framework, this study investigates the possibility of using GAs to define the optimal geometry of lightweight transparent noise screens to be installed on the building façades of urban canyons. This novel approach is applied to a real urban context, *i.e.* the town of Marina di Ragusa, which has been experiencing problems of noise pollution for several years, especially in the summer, due to the high number of recreational activities that are open till late night. In particular, Section 2 presents the mathematical model that is used to predict the sound attenuation introduced by the proposed noise screens, based on the Huygens-Fresnel principle for the diffracted sound component. Then, Section 3 describes the case study, and shows the results of a measurement campaign to quantify the sound pressure level induced by human activities on two receivers, thus demonstrating the urgent need for intervention. Finally, Section 4 presents the results of the optimization process and discusses the consequent strategies needed to improve the acoustic quality of the selected urban area.

2 Methodology

2.1 Mathematical model

In order to assess the effectiveness of a noise screen, it is necessary to introduce a suitable mathematical model to describe all physical phenomena related to sound propagation in an urban canyon. In this paper, the authors use an approach based on geometrical acoustics (*ray-tracing*), where sound waves are regarded as rays interacting with the surfaces; moreover the main sound sources are represented by people chatting along the street.

As depicted in Figure 1, it is possible to identify three different components contributing to the sound pressure

level perceived by the receiver R when the direct path from the point source S is occluded by a noise screen, *i.e.* reflected, transmitted and diffracted sound.

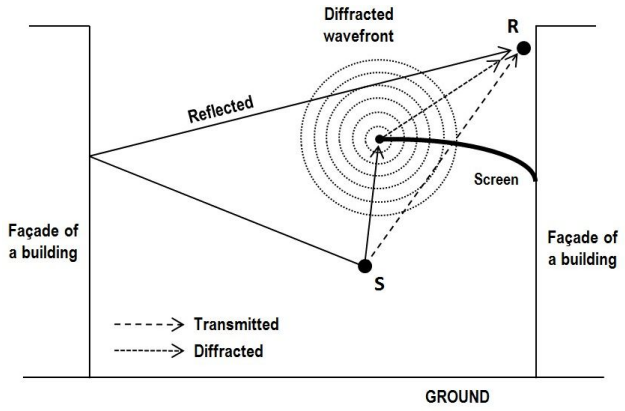

Figure 1: Simplified sketch of the sound components reaching a receiver

However, the sound transmission through the screen can be assumed negligible if compared to the contribution of reflected and diffracted sound waves, especially if the screen is sufficiently stiff. Moreover, the transmitted component would not play an important role during the optimization process for the shape of the screen, which is the focus of this paper, because it only depends on the choice of the material, and not on the geometry. With reference to Figure 1, people are considered as isotropic point sources (IPS) emitting spherical sound waves, hence the same sound energy can be associated to each ray emitted by the source.

Once the path of a ray is traced, it is possible to calculate the attenuation of the sound pressure level according to the theory of sound propagation in free-field conditions. For each octave band from 125 Hz to 4000 Hz, the expected direct sound pressure level ($L_{p,d}$) at a receiver is given by:

$$L_{p,d,j} = L_{W,j} - 20 \cdot \log(r_d) - 11 \quad (1)$$

Here, $L_{W,j}$ is the sound power level of the source in the considered octave band, and r_d is the distance between the source and the receiver. The contribution of the direct sound is relevant only if the direct path between source and receiver is not occluded by the noise screen.

Equation (1) assumes that the point source is not close to the ground, which is true for the human mouth. Moreover, sound absorption in air is neglected, since this becomes relevant only for high distances and limited to high frequencies [26]. As an example, Kang shows that sound attenuation for air absorption at a distance of 20 m is around 1 dB at 4000 Hz when the outdoor temperature is 20°C and the relative humidity is 40-50% [27], and even less at lower frequencies. This justifies the common praxis to neglect this effect in narrow urban canyons, especially when the sound is dominated by medium and low frequencies [28]. Moreover, other meteorological effects, *e.g.* scattering from atmospheric turbulence and refraction due to wind and temperature profiles, are ignored; this is a commonly accepted simplification for line-of-sight propagation in streets, while in case of sound propagation over rooftops these effects should be included [29].

As concerns the reflected component of the sound energy, specular reflection is considered. This means that for every reflected sound wave an image source is introduced; in order to limit the computational effort, only first order reflections are included, that give the most important contribution to the sound level at the receiver.

In fact, as reported by Van der Eerden *et al.* [30], in urban canyons it might be necessary to include at least four reflections to get accurate results from the calculations. However, the same authors specify that the minimum number of multiple reflections required for accuracy purposes is likely to depend on the specific configuration of the urban canyon. Thomas *et al.* also found out that the contribution of the reflected sound waves to the sound pressure level measured on a façade mainly depends on the width of a street, while the height of the buildings and the roughness of their façades only have a minor role [31]. In the present study, an attempt has been made to include up to the third reflection: due to the width of the street and to the presence of several balconies shielding the receivers, the deviation from simplified model is below 1 dB despite the higher computational effort, which justifies the proposed simplification.

Under these assumptions, the sound pressure level associated to the reflected component can be calculated similarly to the direct component, but the total distance run by each reflected ray (r_r) from the image source to the receiver must now be considered:

$$L_{p,r,j} = L_{W,j} - 20 \cdot \log(r_r) - 11 + 10 \cdot \log(\rho) \quad (2)$$

Here, ρ is the sound reflectance of the reflecting surface. All common outer finishing materials (plaster, stones, bricks, windows) show very high sound reflectance ($\rho >$ 0.9) for all octave bands [29]. In this paper $\rho = 1$ is considered, which allows to partially compensate for the small inaccuracy due to the inclusion of the only first reflection. It is also necessary to underline that modeling sound reflection as specular is not rigorous for high frequencies, that is to say when the wavelength is comparable to the size of the irregularities on the façade [29]. In this case, scattered (dif-

fuse) reflection should be considered, which would attenuate the sound energy transferred to the receivers [27]: here again, the hypothesis of specular reflection partially compensates for the underestimation due to ignoring other reflections than the first one.

Finally, the diffracted component is modelled with reference to the Huygens-Fresnel principle, based on the assumption that, for a given point source, every point belonging to the primary wavefront can be thought of as a secondary emitter that generates a new (secondary) wavefront in phase and with the same frequency as the primary one. At any moment, the sound energy reaching a receiver can be calculated as the combination of the sound energy coming from all the secondary emitters, corrected through an *obliquity factor*. This is defined as in Eq. (3), where Θ is the angle between the normal to the primary wavefront and the direction aiming at the receiver (from the secondary source):

$$K(\theta) = 0.5 \cdot (1 + \cos\theta) \tag{3}$$

Starting from this principle, Kapralos *et al.* [33] set up a geometric construction to estimate the sound energy reaching a receiver (R) from a given point sound source (S) after being diffracted by the edge of a screen. In particular, the energy reaching the receiver at a given time t can be calculated by considering only the secondary emitters that are visible from the same receiver and that belong to the so-called "1^{st} Fresnel zone". This is a ring-like region determined by the intersection of the primary wavefront with a sphere of radius ($r_0 + \lambda/2$), centered in the receiver (see Figure 2).

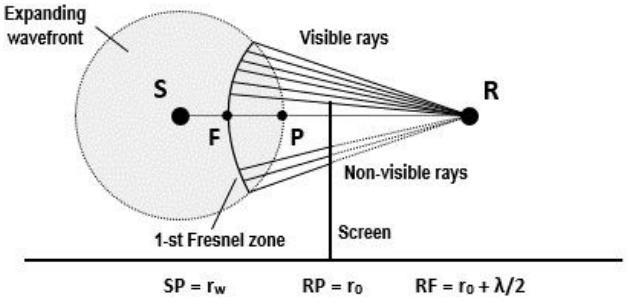

Figure 2: Geometry for the calculation of the diffracted sound pressure at time t

In Figure 2, r_W is the distance run by the primary wavefront at time t, r_0 is the distance between the primary wavefront and the receiver, and λ is the wavelength.

To this aim, they introduced a *visibility factor* v_1 defined as in Eq. (4), where N_{rays} is the total number of rays that can be traced from the 1^{st} Fresnel Zone to the receiver, and N_{vis} is the number of rays actually visible by the receiver:

$$v_1 = \frac{N_{vis}}{N_{rays}} \tag{4}$$

According to this approach, for each octave band the diffracted sound pressure reaching the receiver at time t can be assessed as:

$$p_{diff,j}(t) = v_1 \cdot \frac{K(\theta) \cdot p_{S,j}}{(r_W + r_0)} \cdot \sin\left[\frac{2\pi}{f_j} \cdot t - \frac{2\pi}{\lambda_j} \cdot (r_W + r_0)\right] \tag{5}$$

Here, $p_{S,j}$ is the amplitude of the sound pressure released from the source in the given octave band (Pa); according to Eq. (5), this sound pressure is concentrated in the centre frequency of the band. By using the result of Eq. (5), it is then possible to assess the sound pressure level due to the diffracted component:

$$L_{p,diff,j} = 10 \cdot \log_{10}\left(\frac{1}{T_j}\int_{T_j}\frac{p^2_{diff,j}(t)}{p_0^2}\,dt\right) \tag{6}$$

In Eq. (6) T_j is the period of the sound wave ($T_j = 1/f_j$). Finally, for each octave band the total sound pressure level at the receiver position is the sum of the direct, reflected and diffracted components, according to Eq. (7):

$$L_{p,j} = 10 \cdot \log_{10}\left(10^{\frac{L_{p,d,j}}{10}} + 10^{\frac{L_{p,r,j}}{10}} + 10^{\frac{L_{p,diff,j}}{10}}\right) \tag{7}$$

The direct contribution is not relevant in case of sound sources "hidden" by the noise screens or by the balconies. Equation (7) implies that the energy associated with all the sound waves reaching a receiver can be simply added, without accounting for phase shifts [34]. However, in narrow street canyons this can be acceptable [29]: in this study, given the width of the canyon (around 6 m, as discussed in the next sections), interference effects due to phase shifts occurs only below 63 Hz, *i.e.* out of the range of frequencies considered in the study, where the main sound source is the human voice. The total sound pressure level for the entire spectrum is then:

$$L_p = 10 \cdot \log_{10}\left(\sum_{j\,=\,125\,Hz}^{4000\,Hz} 10^{\frac{L_{p,j}}{10}}\right) \tag{8}$$

2.2 Implementation of the genetic algorithm

2.2.1 General issues

The algorithm created to calculate the noise attenuation produced by the lightweight noise screens, and to optimize their geometry, was developed in a *Rhinoceros 3D™*

environment through the use of the *Grasshopper* plug-in, which allows parametric modelling and supports the resolution through GAs with the *Octopus* add-on, an evolutionary solver [35].

The geometry of the site, including the street, the façades of the buildings and their balconies, can be modelled on Rhinoceros through flat surfaces. It is here necessary to underline the importance of including balconies in the model, which have a non-negligible influence on the noise levels measured on the façade of a building in urban areas. As an example, Mohsen and Oldham [36] demonstrated that a first-floor open balcony with 1 m depth and without a ceiling provide a reduction of the sound pressure level by around 6 dB(A). Balconies at higher floors can give even better protection, *i.e.* up to 7.5 dB(A) at the centre of the back wall and at a height of 1.5 m above the balcony [37].

An algorithm is then developed in order to calculate the sound pressure level expected in the position of the receivers, as a function of the geometry of the buildings and of the noise screens, according to the approach outlined in Section 2.1. In particular, the optimization process has the purpose to minimize the logarithmic mean of the sound pressure levels on the receiver.

The procedure for the construction of the algorithm takes place through the following modules, which will be described in detail in the following sections:

- "Source-receiver" module, to manage the geometry of sound sources and receivers;
- "Screen shape" module, to define analytically shape and position of the noise screens;
- "Sound propagation" module, to manage beam tracing and determine the sound pressure levels, with and without screens;
- "Constraints" module, to check that the solutions comply with all geometric constrains;

The adoption of GAs for optimization implies an iterative process, according to the steps described below:

- Random creation of a first generation of solutions, often characterized by an initial boost, in order to let the algorithm a better exploration;
- Each individual of the generation is evaluated through a fitness function, as explained in Section 2.2.6;
- The algorithm chooses the best solutions;
- Mutation and crossover are operated in order to generate a new class of solutions, starting from the previous ones;
- The new generation is evaluated according to step 2, starting a new iteration.

In this iterative process, many parameters need to be tuned in order to find the best performance. One of these parametrs is the *elitism factor*: elitism is a selection process that implies copying a certain proportion of the fittest candidates, unchanged, from one generation to the following one. In this study, the elitism factor is set to 0.5. Then, one needs to set the *crossover factor*: crossover means that some individuals of a generation are created by exchanging chromosomes of a pair of individuals (parents) chosen from the population, with the possibility that good solutions can generate better ones [38]. In this study, the crossover factor is set to 0.8. Finally, the *mutation probability* must be considered: the mutation operator is used to change some elements in selected individuals, leading to additional genetic diversity to help the search process escape from local optimum traps [38]. In this study, the mutation probability is 0.1.

2.2.2 "Source-receiver" module

The receivers are represented by a mesh of points: the sound pressure levels are calculated for all the points in the mesh, and then the logarithmic mean value is assessed (Figure 3a). In this way, it is possible to investigate the effect of the noise screens over a wider area compared to the case in which the receiver is modelled as a single point.

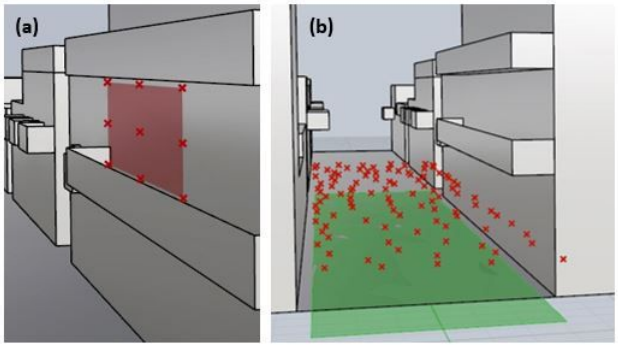

Figure 3: (a) Mesh used for a receiver; (b) Modelling the relevant sources for the receiver

Depending on the location of the receiver, an "influence area" is then selected for the modelling of the sources, *i.e.* that part of the site whose disturbance affects the receiver in question significantly. Subsequently, the area in question is randomly "populated" with point sources, thanks to the Grasshopper *Populate2D* function

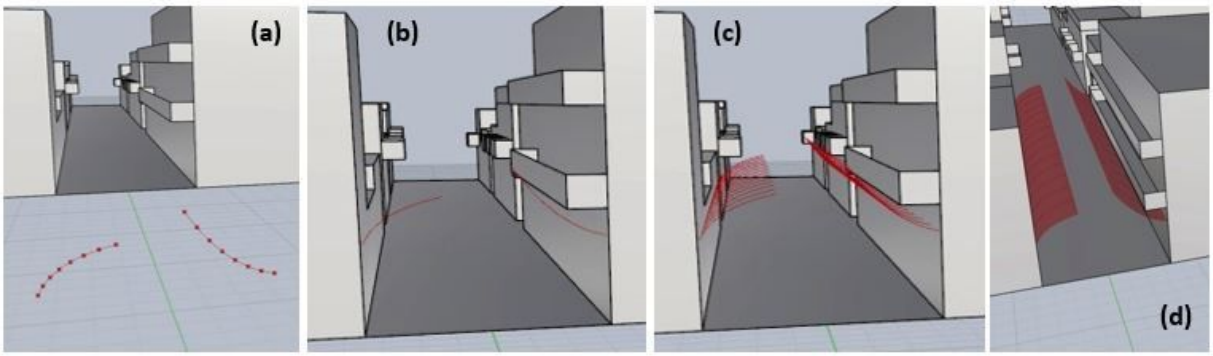

Figure 4: Process to build the geometry of the noise screens. (a) definition of the shape; (b) starting point; (c)-(d) extrusion along the facade

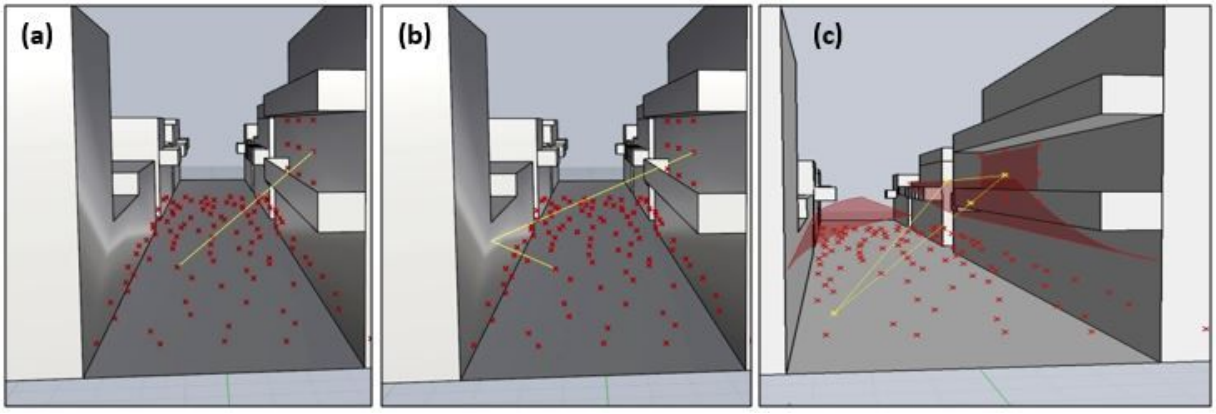

Figure 5: (a) Direct beam; (b) Reflected beam; (c) Diffraction according to Huygens-Fresnel

(Figure 3b). This way of representing the sources introduces in the algorithm the randomness that is typical of the real sources, that is to say people chatting in the street.

2.2.3 Screen shape module

The design of a screen follows three steps, namely defining the shape of the screen by a mathematical equation (Figure 4a), identifying the starting point on the façade (Figure 4b) and defining the length of the screen along the facade (Figure 4c and Figure 4d).

The possibility to describe the shape of the noise barriers through a mathematical equation can lead to interesting practical applications. As an example, the equations can be used as an input to 3D printers in order to build the noise screen profiles with plastic transparent materials.

2.2.4 Sound propagation module

The "Sound propagation" module processes the acoustic modelling to calculate the insertion loss of the noise screens. As a first operation, the algorithm performs the geometric construction of direct and reflected beams linking each receiver to all point sources: direct rays are obtained by linking sources and receivers through a straight line, while reflection is considered up to the first order, and coming only from the façade opposite the position of the receiver (Figure 5). Consequently, the algorithm calculates the sound pressure level associated with each source-receiver pair for octave bands, according to Eq. (1) and Eq. (2).

Then, the algorithm calculates the sound pressure level due to diffraction by the noise screens, according to the approach described in Section 2.1. This algorithm interfaces with another procedure aimed to identify those direct rays that can be intercepted by the noise screens, needed to determine the Fresnel zones. In particular, the procedure consists in:

1. Verification of the diffraction conditions;
2. Construction of two spheres, one representing the primary wave front originating from the source, and the other centered in the receiver: the intersection

of these two spheres determines the 1^{st} Fresnel zone (Figure 2);
3. Identifying eight secondary sources on the Fresnel zone: this number is a good compromise to reduce the calculation time. In fact, the lower is the frequency, the higher is the number of secondary sources needed for a detailed modeling of the Fresnel zone. However, as witnessed by the measured mean pressure level for the noise sources (see Section 3.2), the contribution of the low frequencies – especially 125 Hz – is practically negligible if compared to medium-to-high frequencies, and it would be even lower after the A-weighting filtering. Hence a lower precision of the model at 125 Hz can be accepted.
4. Beams are traced from these secondary sources to both the primary source and the receiver;
5. Checking whether the beams traced in step 4 are obstructed by the shield or by the surfaces of the façades and of the street;
6. Calculating the visibility factor, that depends on the number of obstructed or unobstructed rays, and the diffracted sound pressure reaching the receiver.

Finally, the algorithm calculates the overall sound pressure level detected by the receiver, taking into account only the direct and reflected components that are not intercepted by the shields, plus the diffracted component. The overall sound pressure level for each receiver is determined both in the absence and in the presence of noise screens.

2.2.5 Constraints module

The "Constraints" module checks, during the random generation of solutions, if the individuals selected by the genetic algorithm are admissible configurations. In particular, the module checks that noise screens do not intersect each other and do not intersect the building façades or balconies; moreover, the width of the screen must not exceed a maximum value (*e.g.* 4.5 m) and the noise screens must be placed at least at the height of 2.5 m above the ground. A penalty value is assigned to an individual whenever a constraint is not met, thus helping the algorithm to exclude the individual from the possible set of solutions, as explained in the next section.

2.2.6 Optimization module

The purpose of the genetic algorithm is to minimize the logarithmic mean sound pressure level at the receiver position after inserting the noise screens. However, the algorithm might select solutions leading to this target, but actually either physically impossible or undesired, as the geometric constraints are not met. In order to discard such solutions, the fitness function is defined according to the following expression:

$$\text{Fitness} = \overline{L_p} + \gamma \cdot \sum_{k=1}^{n} p_k \tag{9}$$

Here, L_p is the logarithmic mean of the sound pressure levels calculated on the receiver mesh, γ is a penalty value and p_k is a binary parameter that takes the value 1 when one out of the n possible constraints is not met. An arbitrarily high value is assigned to the penalty (γ = 30 dB), which is sufficient to make the fitness function too high if only one constraint is not met, thus leading to discarding the corresponding solution.

3 Case study

3.1 Description of the selected area

Marina di Ragusa is a small town in the southern coast of Sicily. Following the opening of the tourist port, Marina di Ragusa was affected by intense actions of renewal of the urban setting, in order to receive major tourist flows. In particular, the whole area between the port and the city centre was involved in renovations, by enlarging the promenade and closing it to the traffic.

Consequently, the downtown has become attractive for pubs, wine bars, restaurants and other recreational activities, turning from a residential area into the core of the urban life, especially in the summer. Indeed, in this season the population of Marina di Ragusa grows from around 3,000 people to more than 30,000 people.

However, the tourist and economic development of the city centre of Marina di Ragusa contrasts with the previously quiet residential context: the high number of restaurants and public places attract users until late at night, thus disturbing the peace of residents.

With the aim to reduce the adverse effects of noise pollution and to guarantee the environmental sustainability of urban areas, several rules are foreseen in the EU countries. Specifically, in Marina Ragusa the Mayor's ordinance "Regulations about noise emissions and measures

Figure 6: Tindari Street in daytime (on the left) and nighttime (on the right)

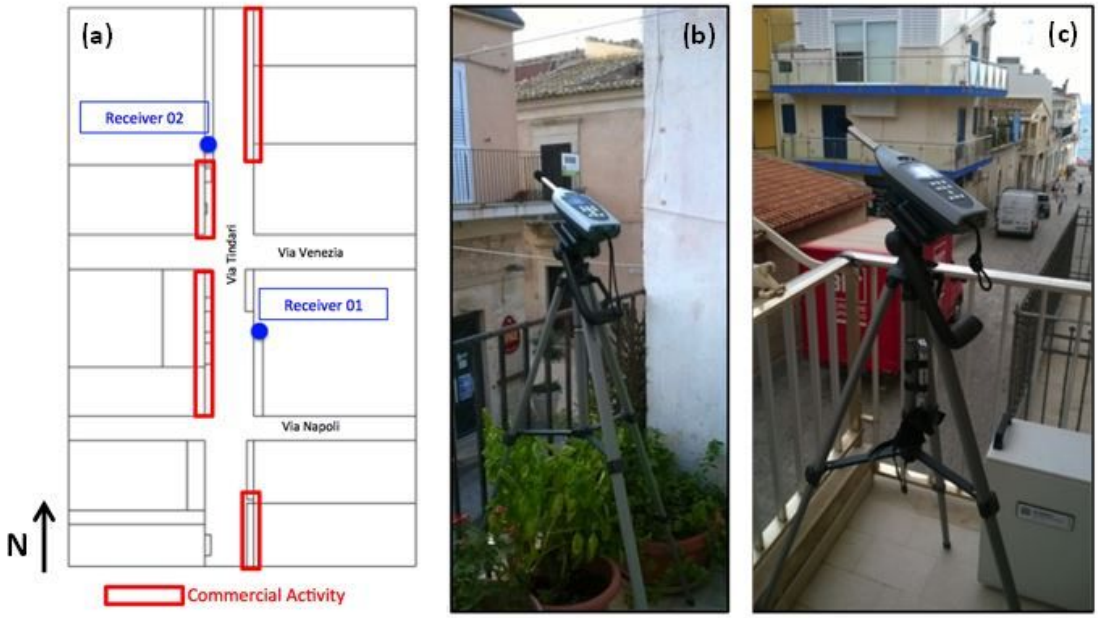

Figure 7: (a) Positions for the noise measurement sessions; (b) Receiver 01; (c) Receiver 02

regarding urban security" has introduced the obligation to comply with the noise emission limits indicated in the Prime Minister Decree (D.P.C.M.) of 14 November 1997 [39], and the conclusion of every music performance at 1.00 am (2.00 am on Saturdays). In particular, Tindari Street (Figure 6) has become the symbol of the transformation of Marina di Ragusa, as the place where the highest number of new businesses has been opened in the last decade. Hence, this street, that is about L = 50 m in length and D = 6 m in width, was chosen as an emblematic case study of noisy densely built areas. The height of the buildings ranges from H = 5 m to H = 8 m, meaning that the height-to-width ratio (H/D) for the urban canyon is around 1.

3.2 Noise measurements

The measurement of the noise pollution in a site is an essential step to plan possible mitigation actions. Hence, in order to assess the sound pressure level occurring during an average summer night in Tindari street, two noise measurement sessions were carried out at two positions, identified as Receiver 01 and Receiver 02, on the balconies of two buildings located along the street (Figure 7). During the measurement sessions, the crowd was uniformly spread along the entire street, as observed in Figure 6.

The measurement of the sound pressure level was performed according to the ISO 1996 international standard [40, 41]. The equipment consists of an integrating Class 1 sound level meter (01dB SIP_95), a calibrator (01dB

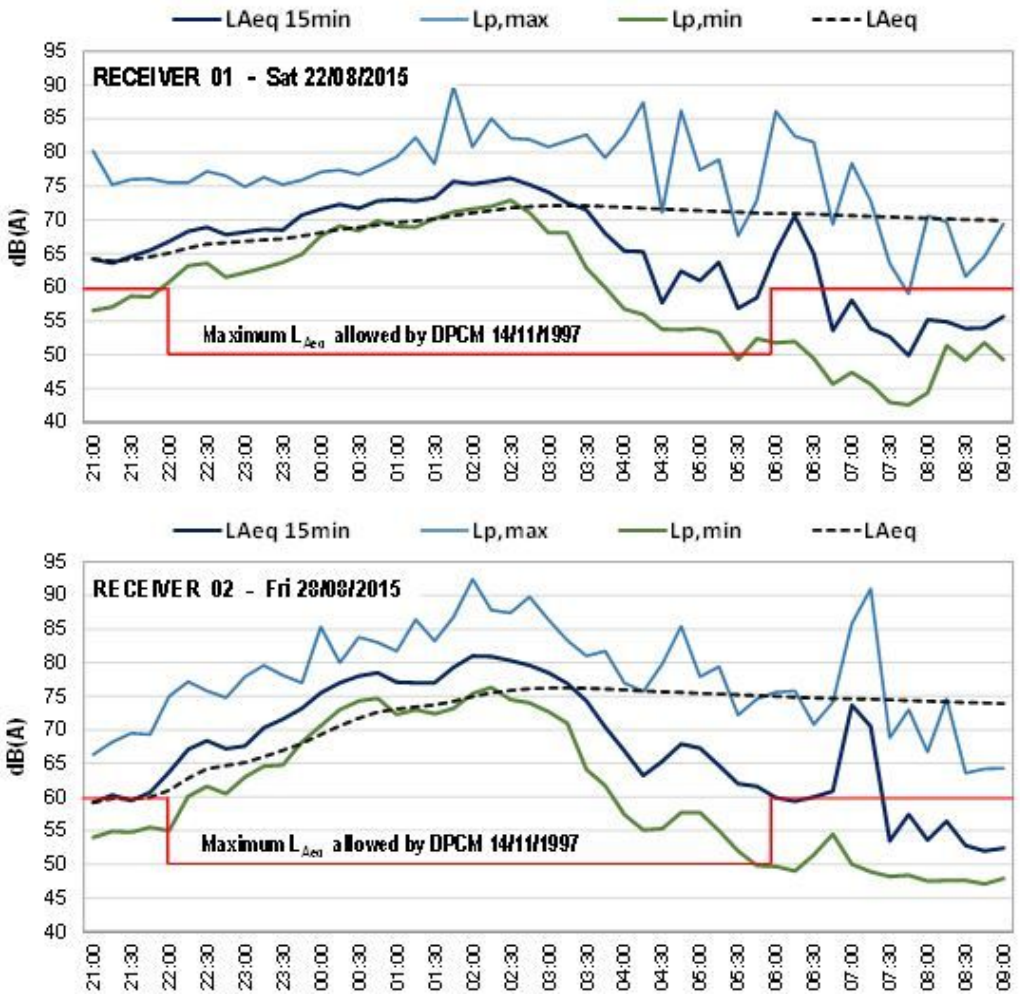

Figure 8: Results of the noise measurement campaign for Receiver 01 and Receiver 02

CAL21), a software tool for sound post-processing (01dB dBTrait) and a digital audio recorder.

The sound level meter was placed at the height of 1.5 m above the level of the balcony, one meter away from the façade. The measurements were performed between 21:00 and 09:00 on Saturday night (22 August 2015) for Receiver 01, and on Friday night for Receiver 02 (28 August 2015). In both cases, Tindari street was very crowded till late night, as usual almost every day in summer, and especially from Friday to Sunday.

During the measurement sessions, in addition, an audio recording was carried out in order to analyse the sound frequency spectrum and to identify the origin of each sound event.

The time interval was set to 15 minutes, meaning that every 15 minutes the minimum ($L_{p,min}$) and the maximum ($L_{p,max}$) sound pressure level, as well as the equivalent continuous sound pressure level (L_{Aeq_15min}), were logged. The latter is the level of a continuous steady sound that, within the same time interval Δt, has the same effective sound pressure as the measured sound, calculated as:

$$L_{Aeq\_15\,\mathrm{min}}(t) = 10 \cdot \log_{10}\left[\frac{1}{\Delta t} \cdot \int_{\Delta t} \frac{p_A^2(t)}{p_0^2} dt\right] \qquad (10)$$

Here, p_A is the A-weighted running value of the sound pressure, and p_0 = 20 μPa is the reference sound pressure. Figure 8 shows the trend of the above parameters, together with the *running cumulative equivalent sound pressure level*, the latter being defined as in Eq. (2), where t_0 is the start of the measurement campaign:

$$L_{Aeq}(t) = 10 \cdot \log_{10}\left[\frac{1}{(t - t_0)} \cdot \int_{t_0}^{t} 10^{\left(\frac{L_{Aeq\_15\,\mathrm{min}}(t)}{10}\right)} dt\right] \qquad (11)$$

The diagram also shows the limit value of the L_{Aeq} allowed by *D.P.C.M.* 14 November 1997 for the selected area, that are 50 dBA at night (22:00 - 6:00) and 60 dBA during daytime (6:00 - 22:00).

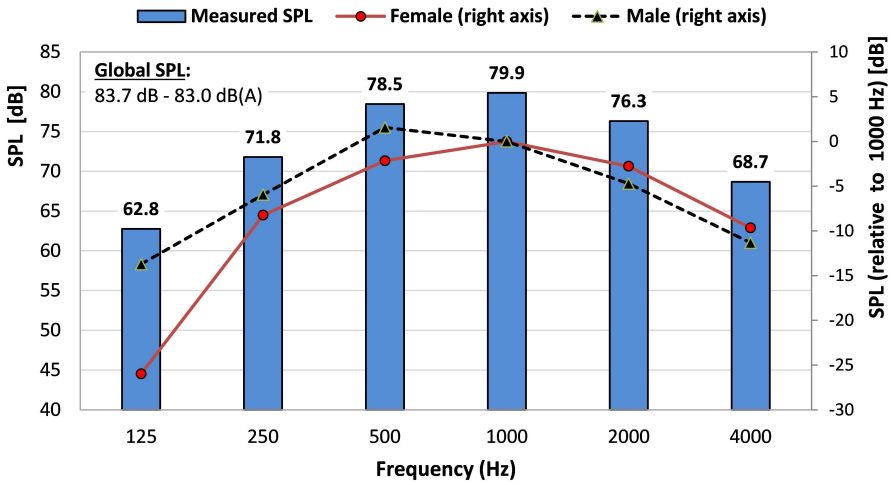

Figure 9: Mean sound pressure level at 1 m from small groups of people, as measured in Tindari street. The figure also shows the relative voice spectra for people speaking at loud voice level (adapted from reference [42])

Although the measurements were carried out during two different nights, in both positions it is possible to observe the same trend: increasing sound pressure levels are measured from 21:00 to 02:00, then the values keep almost constant between 02:00 and 03:00, and finally they decrease until 04:00.

The highest noise levels are detected between 02:00 and 03:00, that is to say when music events are not authorized. However, it should be noted that restaurants and clubs still keep open after 3:00 a.m., thus contributing to noise because of the customers who stay in the street.

In order to characterize the sources of disturbance that are active during the measurement period, the authors have verified the audio recorded during the second session of measurement. Different sources can be distinguished, according to the following periods:

- **22:00-23:00:** music is the predominant source;
- **23:00-01:30:** the noise increases, as both the volume of music and the noise made by people increase;
- **01:30-04:30:** the noise made by people is predominant. Music can be heard until 3:30;
- **04:30-07:00:** people are still present. Pubs and nightclubs are closing. Some noise is made for removal of garbage, mainly the management of glass bottles;
- **07:00-07:30:** street cleaning service.

If looking at the values of the sound pressure levels, in the position of Receiver 01 three peaks were detected: 89.7 dB(A) between 01:30 and 02:00, 87.4 dB(A) and 86.2 dB(A) between 04:00 and 05:00. The peak sound pressure levels for Receiver 2 are even higher, and can exceed 92 dB(A). Moreover, in the position of Receiver 02, L_{Aeq_15min} shows much higher values than for Receiver 01, *i.e.* beyond 80 dB(A) between 02:00 and 02:30, because the receiver is very close to the most popular pubs, where most of the clients gather.

The sound pressure levels are below the limits specified in the *D.P.C.M.* of 14 November 1997 only after 06:30, when the limit is 60 dB(A) for daytime. During the rest of the time, and at nighttime in particular, the limit is widely exceeded with deviations higher than 20 dB(A). Finally, a statistical analysis of SPL shows values of L_{95} (that is, the sound pressure level exceeded for 95% of the measurement time, referred to each period of 15 minutes) recurrently above 70 dB(A).

Finally, one last short measurement campaign was performed in order to assess the average sound pressure level close to the sound sources. In this context, a sound source can be identified as a small group of people chatting outdoors. To this aim, the sound level meter was placed in Tindari street at a distance of 1 m from several small groups of people in the night of 22 August 2015 (Saturday). The average sound level spectrum resulting from this survey is reported in Figure 9; the figure also shows average voice spectra for small group of talkers speaking at loud voice level (please note that these spectra are relative to the sound pressure level measured at 1000 Hz), as reported in a study from the US Environmental Protection Agency [42]. The frequency distribution of the measured sound pressure level for the human voice is coherent with the curves available in the literature, where loud vocal emissions are concentrated between 500 Hz and 2000

Hz for both males and females, while they steeply decrease in the other frequencies.

The results discussed above highlight the need to adopt measures to reduce the noise perceived by the residents, which are severely disturbed and almost unable to sleep at night. One might argue that the sound pressure levels were measured outdoors, and not inside the apartments; however, in this area it is a very common habit in the summer to keep windows open at night while sleeping, due to the high indoor temperature, in the attempt to exploit natural ventilation. This means that the expected sound pressure levels inside the apartments will be very close to what is measured on the balconies.

One of the possible actions to mitigate noise disturbance to the residents is the use of lightweight transparent noise screens, which might be installed on the building facades without altering the visual context. Prospective polymeric materials for such applications are Ethylene Tetrafluoroethylene (ETFE), Polycarbonate and Plexiglas.

3.3 Rhinoceros model

The geometry of the site, including the street, the façades of the buildings and their balconies, were modelled on Rhinoceros through flat surfaces (Figure 10).

The potential receivers were placed in the same positions as those used during the sound level measurements. Each receiver is represented by a mesh of nine points with two-metre spacing: the sound pressure levels are calculated for all the points in the mesh, and then the logarithmic mean value is assessed (Figure 3a).

To each receiver a "pertinence area" is assigned, where a series of point sources is arranged randomly. Each point source can be regarded as a small group of people, and is assigned a sound power level that generates, at a distance of 1 m, exactly the sound level spectrum determined through the sound measurements (Figure 9). One hundred point sources are considered for the calculations, which is a compromise between calculation time and emission uniformity in the area of influence in question.

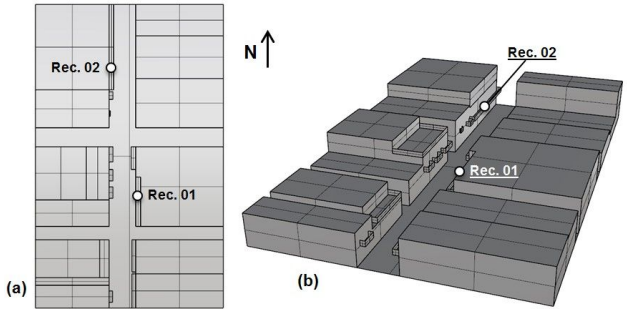

Figure 10: Geometry of the site modelled in Rhinoceros. (a) Plan; (b) Perspective

3.4 Noise screen shape

The noise screens are applied to both the building façades facing the street. The noise screens are made of multiple two-meter wide modules, which can have different shapes on the two sides of the street. The noise screens were modelled according to three possible geometries, namely linear, parabolic and logarithmic spiral shape, each defined through a parametric equation.

This means that each profile is described by an equation written with reference to a local coordinate system, whose origin is set on the façade at a certain height h above the ground. Table 1 reports the equations used to plot the profiles, where t is a progressive parameter, ranging from 0 to 1, needed to identify eight points on the profile (one point at every step Δt = 1/7). Figure 11 shows some examples with the values of the corresponding parameters.

Moreover, the local coordinate system can be rotated around a straight line containing the origin and lying on the façade: the rotation angle θ is measured (in radians) between the x-axis of the local coordinate system and the normal to the façade. The angle can be greater than π for the screens on the opposite side, meaning that the direction of these screens is reversed.

Overall, the definition of the geometry and the position of a profile needs a series of data, namely the parameters to define the equations (A, B, C), the rotation angle θ, the height h above the ground, the number of modules to be used (each module being two-meter wide) and the distance of the first module from the corner of the building.

Each parameter can be configured independently for each noise screen. All the parameters listed so far build the genome needed for the solution of the problem through genetic algorithms.

4 Results and discussion

4.1 Optimum shape and corresponding insertion loss

Table 2 and Table 3 report the parameters identifying the optimum screen configurations, *i.e.* the shapes of the screens that allow minimizing the mean sound pressure levels perceived by the receivers. For each receiver, two

Table 1: Geometric features of the profiles chosen for sound shields

Profile type	Equation in *x*	Equation in *z*	Parameters of the profile
Linear	$x = B \cdot t$	$z = B \cdot t$	B: scale factor
Parabolic	$x = B \cdot t$	$z = C \cdot A \cdot t^2$	A: width of the parabola B: scale for the x-axis C: direction of concavity (C = ± 1)
Logarithmic spiral	$x = C \cdot A \cdot e^{B \cdot T} \cdot \cos(t)$	$z = A \cdot e^{B \cdot T} \cdot \sin(t)$	A: width of the spiral B: scale factor C: direction of the spiral (C = ± 1)

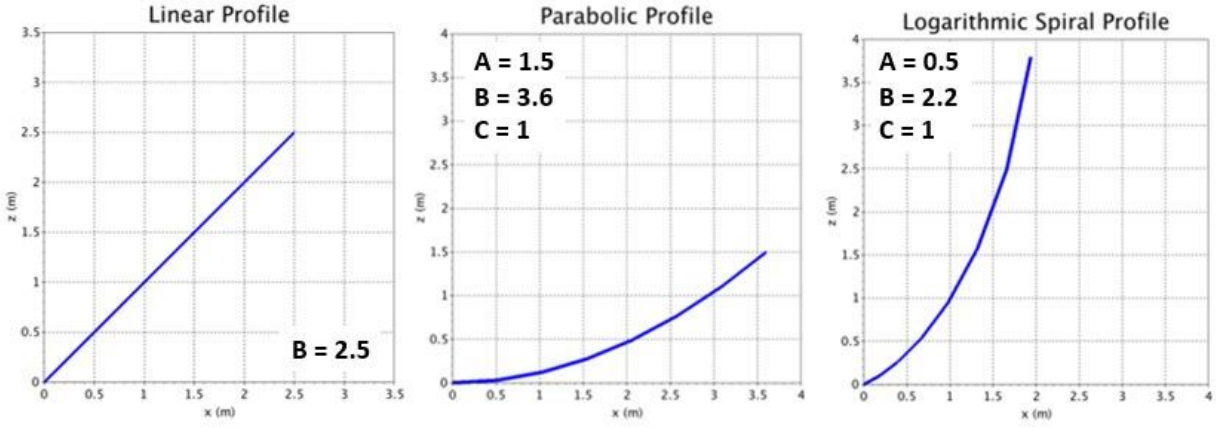

Figure 11: Examples of possible screen profiles, with their corresponding parameters

Table 2: Optimum screen configuration for Receiver 01

	Linear		Parabolic		Logarithmic Spiral	
	Screen 1	Screen 2	Screen 1	Screen 2	Screen 1	Screen 2
Equation parameters	B = 2.2	B = 2.3	A = 0.4 B = 3.8 C = 1	A = 2.2 B = 1.6 C = 1	A = 0.2 B = 3.0 C = 1	A = 0.4 B = 2.2 C = −1
Rotation angle	4.6 rad	0.5 rad	3.7 rad	0.4 rad	4.3 rad	2.2 rad
Height above ground	2.6 m	3.1 m	3.0 m	2.8 m	3.3 m	3.1 m
Number of modules (2 m each)	7	3	9	4	8	9
Distance from the edge	6.3 m	15.2 m	4.9 m	11.9 m	6.9 m	4.4 m

Table 3: Optimum screen configuration for Receiver 02

	Linear		Parabolic		Logarithmic Spiral	
	Screen 1	Screen 2	Screen 1	Screen 2	Screen 1	Screen 2
Equation parameters	B = 3.0	B = 0.8	A = 0.8 B = 3.6 C = 1	A = 3.8 B = 1.9 C = 1	A = 0.6 B = 1.9 C = 1	A = 3.5 B = 0.2 C = −1
Rotation angle	0.5 rad	3.6 rad	6.0 rad	4.4 rad	6.7 rad	5.1 rad
Height above ground	3.5 m	2.9 m	2.9 m	2.6 m	2.7 m	2.6 m
Number of modules (2 m each)	16	16	15	11	16	6
Distance from the edge	1.4 m	0.4 m	1.6 m	8.7 m	0.9 m	19.7 m

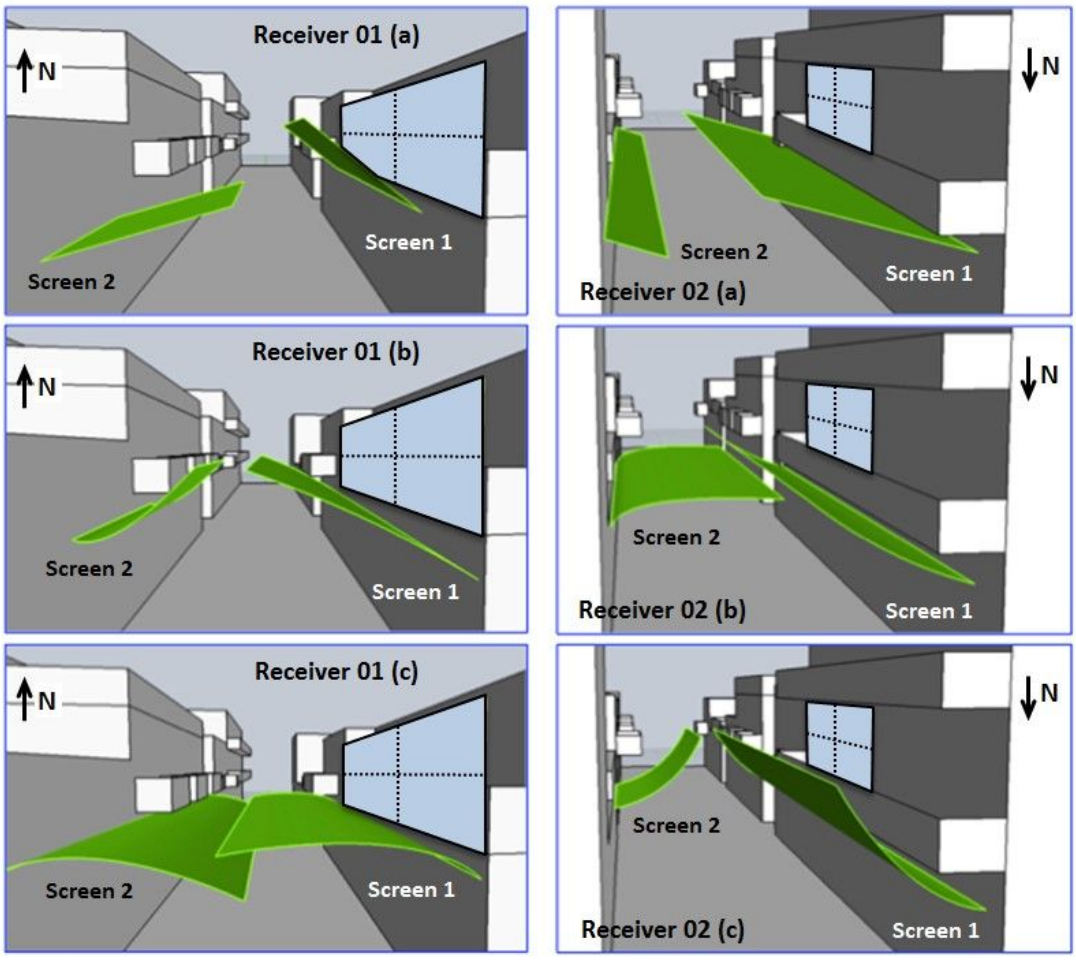

Figure 12: 3D view of the best configurations for linear (a), parabolic (b) and logarithmic spiral (c) screens in relation to Receiver 01 (on the left) and Receiver 02 (on the right)

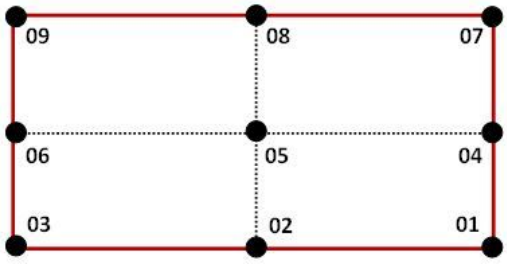

Figure 13: Identification of the points in the mesh for the generic receiver

screens are installed: screen 1 is the one placed below the receiver itself, while screen 2 is placed on the opposite side of the street. Figure 12 shows the corresponding shapes and their position on the façades in the 3D view built in Rhinoceros; the two receivers are observed from two opposite sides of Tindari street. In particular, Receiver 01 is observed from the Southern end of the street, and Receiver 02 from the Northern end.

Finally, Table 4 and Table 5 show the A-weighted sound pressure level predicted for each point of the mesh used for the simulation of Receiver 01 and Receiver 02 (see Figure 13), together with the logarithmic mean sound pressure level over the whole receiver. The values refer both to the situation without noise screens and to the optimum screen configuration, according to the three possible shapes. The insertion loss (IL) corresponds to the difference between the sound pressure levels measured without and with the screens.

First of all, one can observe that the average sound pressure level without noise screens (76.5 dB(A) in Receiver 01 and 75.4 dB(A) in Receiver 02) is very close to the values of the equivalent continuous sound pressure level (L_{Aeq_15min}) measured on-site and reported in Figure 8. Of course a direct comparison is not possible, since the actual sound sources (*i.e.* people chatting and shouting) have an

Table 4: Sound pressure level with and without noise screens: Receiver 01. All values in dB(A)

Point	No screen	Optimum shield profile Linear		Parabolic		Logarithmic	
	L_p	L_p	IL	L_p	IL	L_p	IL
01	77.0	77.0	0.0	73.9	3.1	74.5	2.5
02	77.5	72.6	5.0	71.8	5.7	70.5	7.0
03	77.8	73.8	4.0	71.7	6.1	74.1	3.8
04	75.7	75.3	0.4	71.5	4.3	72.0	3.8
05	76.6	66.6	10.0	66.1	10.5	68.1	8.5
06	76.8	70.0	6.8	69.4	7.4	72.6	4.2
07	74.8	73.7	1.1	70.0	4.7	70.8	4.0
08	75.7	66.2	9.6	65.3	10.5	66.7	9.1
09	75.9	70.9	5.0	70.5	5.5	71.4	4.6
Overall	**76.5**	**73.5**	**3.0**	**70.7**	**5.8**	**71.8**	**4.7**

Table 5: Sound pressure level with and without noise screens: Receiver 02. All values in dB(A)

Point	No screen	Optimum shield profile Linear		Parabolic		Logarithmic	
	L_p	L_p	IL	L_p	IL	L_p	IL
01	76.3	68.4	7.9	67.8	8.5	67.8	8.5
02	76.4	69.6	6.8	68.0	8.4	69.9	6.4
03	76.3	69.2	7.1	68.5	7.8	69.8	6.5
04	75.3	63.0	12.3	58.0	17.3	62.1	13.1
05	75.3	61.9	13.5	56.4	18.9	59.7	15.6
06	75.3	65.9	9.4	63.4	11.9	63.9	11.4
07	74.3	64.2	10.1	66.0	8.4	64.0	10.3
08	74.5	63.4	11.1	63.9	10.6	63.5	11.0
09	74.5	64.1	10.4	64.4	10.1	61.9	12.5
Overall	**75.4**	**66.4**	**9.0**	**65.5**	**9.9**	**66.1**	**9.3**

highly non-stationary character, both in terms of position and sound emission level. However, the good accordance of the results indicates that the adopted representation of the sources, as well as the calculation method, can be reliable for a preliminary design approach.

Now, starting from Receiver 01, it is possible to observe that the linear shape provides the lowest average Insertion Loss (IL = 3 dB), followed by the logarithmic profile (IL = 4.7 dB) and the parabolic shape (IL = 5.8 dB). In fact, from Figure 12 it seems that the optimum linear configuration found by the genetic algorithm does not allow protecting the right-hand side of the receiver, corresponding to the points 01, 04 and 07 (Figure 13), from the noise coming from the southern end of the street. Consequently, in these points the attenuation is very low, ranging from 0 dB to 1.1 dB (Table 4), which penalises severely the overall effectiveness of the screen.

Actually, this is typical a case where the optimization algorithm might have run into a "local optimum", which is not the overall best solution. However, if forcing the algorithm to introduce further noise screens on the right-hand side of Receiver 01, the logarithmic mean sound pressure level perceived by this receiver would be reduced by less than 0.5 dB, which means that the linear profile would still be the worst solution.

The results reported in Table 5 suggest that the noise screens are more effective for Receiver 2, as the predicted Insertion Loss ranges from IL = 9.0 dB with a the linear profile to IL = 9.9 dB with a parabolic profile. The parabolic profile yields the lowest sound pressure levels on point 05 (56.4 dB(A)), and it is very effective also in relation to point 04 (58.0 dB(A)). Actually, the position of Receiver 02 is more suitable because it is located relatively far from the building corner and from the crossroads, which allows placing larger screens than for Receiver 01, thus protecting

the receiver from the noise coming from both sides. Indeed, as observed in Table 3, the main screen is composed by up to 16 modules, whereas for Receiver 01 only 7 to 9 modules are used (Table 2).

Generally, for both receivers the attenuation allowed by the noise screens is more evident in the central zone of the receiver (points 05 and 08), but the favourable position of Receiver 02 introduces a good effectiveness also in the right-hand side of the mesh (point 04). The shape of the secondary screen, whose main aim consists in protecting the receivers from reflected sound waves, is in some cases similar to the main screen. The linear secondary screen has a short profile, since the main screen has already a good extension.

4.2 Discussion

In light of the results discussed in the previous section, it is possible to state that the best shape for the noise screens is the parabolic profile. What makes the parabolic shape the winning solution is the possibility to control the geometry independently on both axes. Figure 14 shows the 3D view of Tindari street with the optimum parabolic noise screens installed on both receivers.

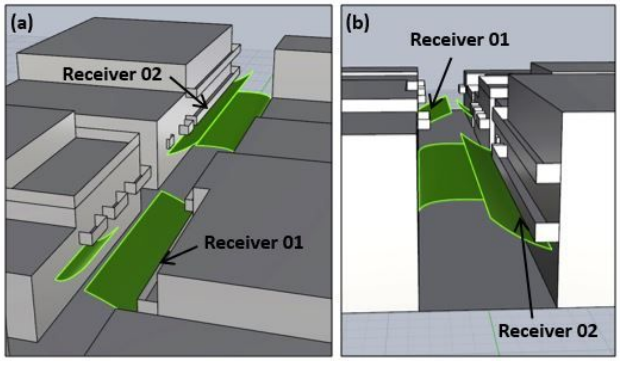

Figure 14: View of Tindari street with optimum parabolic profiles. (a) South-East view; (b) North view

The logarithmic spiral shape, although acoustically performing, is not fully satisfactory because of the excessive width of the profiles. As shown in Figure 12, this makes them invasive, especially for Receiver 01, meaning that they introduce a sharp physical separation between the spaces at the street level and the upper floors. In this case, several side effects can take place:

- noise reverberation, which generates the increase of the sound pressure level perceived by people staying in the street;
- hindrance to the air circulation at street level: heat and pollutants emitted by the customers of the recreational activities can hardly move upwards and leave the urban canyon;
- since the screens absorb the solar radiation, they might get overheated in the daytime, and then transfer radiant heat downwards, making the perceived mean radiant temperature increase consistently.

In this direction, other constraints can be introduced in the genetic algorithm. As an example, the screens can be configured so as not to invade a central strip of the street, whose width might be set to *e.g.* two meters. One more constraint might correspond to a maximum size of the screen, in order to limit its weight and the wind action. In any case, suitable solutions to connect the screens to the façade, thus ensuring their bearing capacity, must be defined in the design stage that will follow this preliminary sizing exercise.

Moreover, the results have shown that the attenuation is very high in some points of the mesh (10.5 dB in point 05 and point 08 for Receiver 01, 18.9 dB and 17.3 dB respectively in point 05 and point 04 for Receiver 02), but it gets much lower in other points of the mesh. Hence, one may decide to set a maximum sound pressure level for every point of the mesh of the receiver, which would lead to a different optimum geometry.

Finally, the proposed procedure allows defining a different shape for the various screens, in order to reduce the sound pressure levels in every single receiver. This means that further screens might be added to other buildings in order to shield all the potential receivers in the street: their shape would be potentially different from that of the screens designed in this study, and further constraints could be possibly introduced in the genetic algorithm in order to ensure a certain uniformity in the shape of all screens, if needed.

One of the limitations of this model is the approximation that sound reflection is purely specular on all surfaces and that roughness of the façades only has a minor role. However, this can be reasonably assumed in the range of mid frequencies (500-1000 Hz), which in this case are the frequencies where the sound emission from the sound sources is mainly concentrated.

5 Conclusions

This study proposes a novel methodology to optimize the design of lightweight transparent noise screens to be installed in urban canyons in order to mitigate environmen-

tal noise, based on genetic algorithms. The methodology is applied to a street in the town of Marina di Ragusa, Southern Italy, which has been experiencing severe problems of noise pollution in the last decade, especially in summer, due to the high number of restaurants and public places open at nighttime.

In a first stage, a noise measurement campaign was performed on site, to understand the extent of the disturbance and to characterize the sources of noise. The noise made by people chatting and shouting in the street turned out to be the main disturbing source in terms of both sound pressure levels and duration.

Subsequently, the geometry of the site was reconstructed in 3D. The prediction of the sound pressure level perceived by the residents is performed in the *Grasshopper* environment where the noise screens were modelled by using three possible shapes: a linear profile, a parabolic profile and a logarithmic spiral profile, built with parametric equations.

The best results were obtained with the parabolic profile solution, with an average Insertion Loss between 6 dB and 10 dB. Possible polymeric transparent materials for such applications are ethylene tetrafluoroethylene (ETFE), polycarbonate and plexiglas, which can be modelled through 3D printers and might be installed on the building facades without altering the visual context.

The study focused just on two selected receivers in order to verify the applicability of the proposed approach. However, it might be extended to all the potential receivers in the street: this would imply the introduction of other screens, whose shape would be independent on that of the screens designed in this study.

The use of genetic algorithms proves to be very effective in the preliminary design stage of a noise screen and allows identifying those shapes that can maximize the Insertion Loss, while meeting the imposed design constraints at the same time. The advantage of this process is thus the possibility to find an optimum solution with a comprehensive approach and a relatively low computational effort. Therefore, the proposed mitigation approach can be applied in urban areas affected by significant noise pollution.

Future development can include the treatment of more complex geometries and the inclusion of other constraints regarding the fruition of the street in terms of ventilation and outdoor thermal comfort. As an example, it would be interesting to investigate the impact of the noise screens on the sound pressure level perceived by pedestrians, in order to understand whether absorption treatments are necessary on the lower side of the screens to avoid excessive reverberation.

Moreover, the methodology can be extended to traffic noise, which is the main source of noise pollution in urban areas.

References

[1] EC Directive, Directive 2002/49/EC of the European Parliament and of the Council of 25 June 2002 relating to the assessment and management of environmental Noise, Official J. Eur. Communities L 189 (2002) 0012-0026 (18.7.2002), Brussels.

[2] WHO Regional Office for Europe, Burden of Disease from Environmental Noise e Quantification of Healthy Life Years Lost in Europe, 2011, ISBN 9789289002295.

[3] Murray Schafer R., The Tuning of the World, 1st ed., Knopf, 1977.

[4] Wang H., Cai M., Luo W., Areawide dynamic traffic noise simulation in urban built-up area using beam tracing approach, Sustain. Cities Soc., 2017, 30, 205–216.

[5] Halperin D., Environmental noise and sleep disturbances: a threat to health? Sleep Science 2014, 7, 209-212.

[6] Ottoz E., Rizzi L., Nastasi F., Recreational noise: Impact and costs for annoyed residents in Milan and Turin. Appl. Acoust. 2018, 133, 173–181.

[7] Ballesteros M.J., Fernández M.D., Flindell I., Torija A.J., Ballesteros J.A., Estimating leisure noise in Spanish cities, Appl. Acoust. 2014, 86, 17–24.

[8] Horoshenkov K., Hothersall D.C., Mercy S.E., Scale modelling of sound propagation in a city street canyon. J. Sound Vib. 1999, 223(5), 795–819.

[9] Baulac M., Defrance J., Jean P., Minard F., Efficiency of noise protections in urban areas: prediction and scale model measurements. Acta Acust. united Ac. 2006, 92, 530–539.

[10] Watts G.R., Crombie D.H., Hothersall D.C., Acoustic performance of new designs of traffic noise barriers: full scale test. J. Sound Vib. 1994, 177, 289–305.

[11] http://proplastik.ee/wp-content/uploads/2015/07/Lexan-PC-murabarjaar.pdf (retrieved on 29/01/2020)

[12] https://www.sheets.covestro.com/index.php/fuseaction/download/lrn_file/mf0326_e_150901.pdf (retrieved on 29/01/2020)

[13] Zuccherini Martello N., Fausti P., Santoni A., Secchi S., The use of sound absorbing shading systems for the attenuation of noise on building façades. An experimental investigation. Buildings 2015, 5, 1346-1360.

[14] Sakamoto S., Aoki A., Numerical and experimental study on noise shielding effect of eaves/louvers attached on building façade. Build. Environ. 2015, 94, 773-784.

[15] Nyuk Hien W., Yong Kwang Tan A., Yok Tan P., Chiang K., Chung Wong N., Acoustics evaluation of vertical greenery systems for building walls. Build. Environ. 2010, 45, 411–420.

[16] Holland J.H., Adaptation in natural and artificial systems, 2nd ed., University of Michigan Press, Ann Arbor, 1992.

[17] Yokota T., Gen M., Taguchi T., Li Y., A method for interval 0-1 nonlinear programming problem using a genetic algorithm. Comput. Ind. Eng. 1995, 29(1-4), 531-535.

[18] Yokota T., Gen M., Li Y., Kim C., A genetic algorithms for interval nonlinear integer programming problem. Comput. Ind. Eng. 1996, 31(3/4), 913-917.

[19] Baulac M., Defrance L., Jean P., Optimisation with genetic algorithm of the acoustic performance of T-shaped noise barriers with a reactive top surface. Appl. Acoust. 2008, 69, 332-342.
[20] Greiner D., Aznárez J.J., Maeso O., Winter G., Shape design of noise barriers using Evolutionary optimization and Boundary Elements, In: Topping B.H.V. *et al.* (Eds.), Proceedings of the Fifth International Conference on Engineering Computational Technology, 2006, 43.
[21] Greiner D., Aznárez J.J., Maeso O., Winter G., Single- and multi-objective shape design of Y-noise barriers using evolutionary computation and Boundary Elements. Adv. Eng. Softw. 2010, 41, 368-378.
[22] Greiner D., Galván B., Aznárez J.J., Maeso O., Winter G., Robust design of noise attenuation barriers with evolutionary multi-objective algorithms and the Boundary Element Method. In: Ehrgott M *et al.* (Eds.), Lecture Notes in Computer Science, Evolutionary Multi-Criterion Optimization, Vol. 5467, Springer, Berlin, Heidelberg, 2009, 261-274.
[23] Grubeša S., Jambrošić K., Domitrovi H., Noise barriers with varying cross-section optimized by genetic algorithms. Appl. Acoust. 2012, 73, 1129-1137.
[24] Deb K., Bandaru S., Greiner D., Gaspar-Cunha A., Celal Tutum C., An integrated approach to automated innovization for discovering useful design principles: case studies from engineering. Appl. Soft Comput. 2014, 15, 42–56.
[25] Toledo R., Aznarez J.J., Maeso O., Greiner D., A procedure for the top geometry optimization of thin acoustic barriers, In: Oate E. *et al.* (Eds.), Proceedings of the 11^{th} World Congress on Computational Mechanic, Barcelona, 2014.
[26] Lamancusa J., Daroux P., Ray tracing in a moving medium with two-dimensional soundspeed variation and application to sound propagation over terrain discontinuities, J. Acoust. Soc. Am. 1993, 93(4), 1716-1726.
[27] Kang J., Numerical modelling of the sound fields in urban streets with diffusely reflecting boundaries, J. Sound Vib. 2002, 258(5), 793–813.
[28] Echevarria Sanchez G.M., Van Renterghem T., Thomas P., Botteldooren D., The effect of street canyon design on traffic noise exposure along roads. Build. Environ. 2016, 97, 96-110.
[29] Hornikx M., Ten questions concerning computational urban acoustics. Build. Environ. 2016, 106, 409-421.
[30] Van Der Eerden F., Graafland F., Wessels P., Basten T., Urban traffic noise assessment by combining measurement and model results, Proc. Meet. Acoust. 2013, 19 (1), 040143.
[31] Thomas P., Van Renterghem T., De Boeck E., Dragonetti L., Botteldooren D., Reverberation-based urban street sound level prediction. J. Acoust. Soc. Am. 2013, 133(6), 3929-3939.
[32] Hornikx M., Forssen J., Noise abatement schemes for shielded canyons. Appl. Acoust. 2009, 70, 267–283.
[33] Kapralos B., Jenkin M., Milios E., Acoustical diffraction modeling utilizing the Huygens-Fresnel Principle. In: Proceedings of HAWE 2005 - IEEE International Workshop on Haptic Audio visual Environments and their Applications, Ottawa, Canada, 2005.
[34] Heutschi K., Calculation of Reflections in an Urban Environment, Acta Acust. united Ac. 2009, 95(4), 644-652.
[35] Mirra G., Pignatelli E., Lucci G., Computational morphogenesis and fabrication of an acoustic shell for outdoor chamber music, Master Thesis, University of Naples “Federico II”, Naples, Italy, 2015.
[36] Mohsen E.A., Oldham D.J., Traffic noise reduction due to the screening effect of balconies on a building façade. Appl. Acoust. 1977, 10, 243–57.
[37] Hossam El Dien H., Woloszyn P., The acoustical influence of balcony depth and parapet form: experiments and simulations. Appl. Acoust. 2005, 66, 533–551.
[38] Lin W.Y., Lee W.Y., Hong T.P, Adapting crossover and mutation rates in genetic algorithms. J. Inf. Sci. Eng. 2003, 19, 889-903.
[39] D.P.C.M. 14/11/1997 Determinazione dei valori limite delle sorgenti sonore (in Italian).
[40] ISO 1996-1, 2016. Acoustics — Description, measurement and assessment of environmental noise. Part 1: Basic quantities and assessment procedures. International Organization for Standardization, Geneva, Switzerland.
[41] ISO 1996-2, 2017. Acoustics — Description, measurement and assessment of environmental noise. Part 2: Determination of sound pressure levels. International Organization for Standardization, Geneva, Switzerland.
[42] Olsen W.O., Average Speech Levels and Spectra in Various Speaking/Listening Conditions: A Summary of the Pearson, Bennett & Fidell (1977) Report, Amer. J. Audiol., 1998, 7(2), 1-5.